How a shower looks like

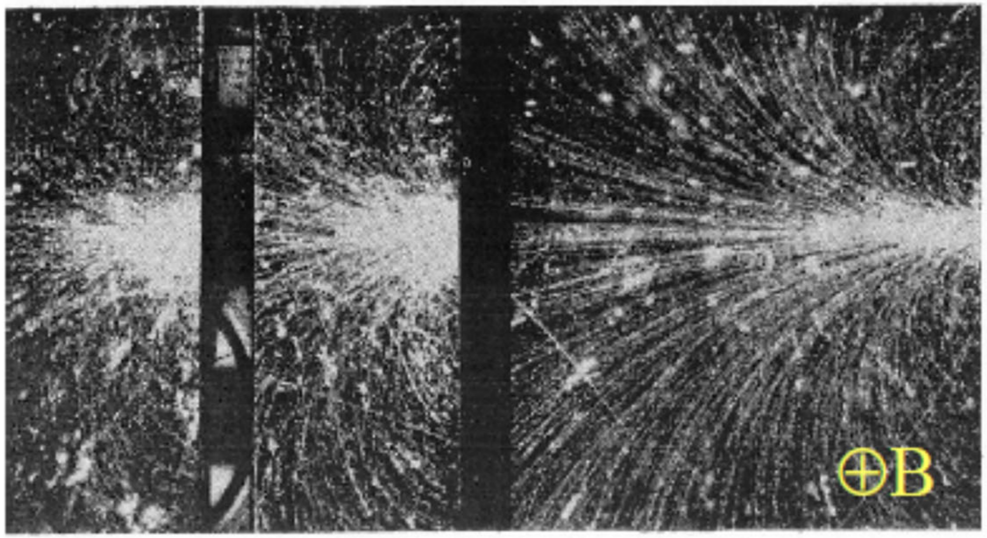

Electron shower in lead. 7500 gauss in cloud chamber. CALTECH

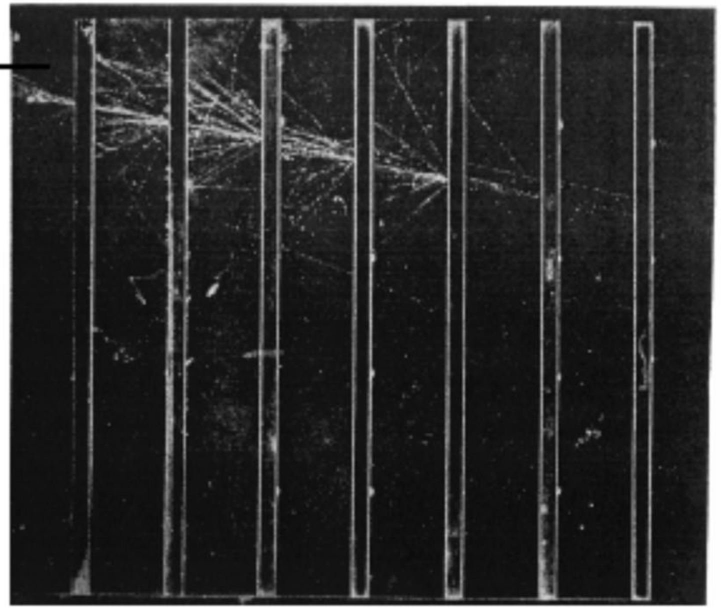

Electron shower in lead. Cloud chamber. W.B. Fretter, UCLA

Electron showers

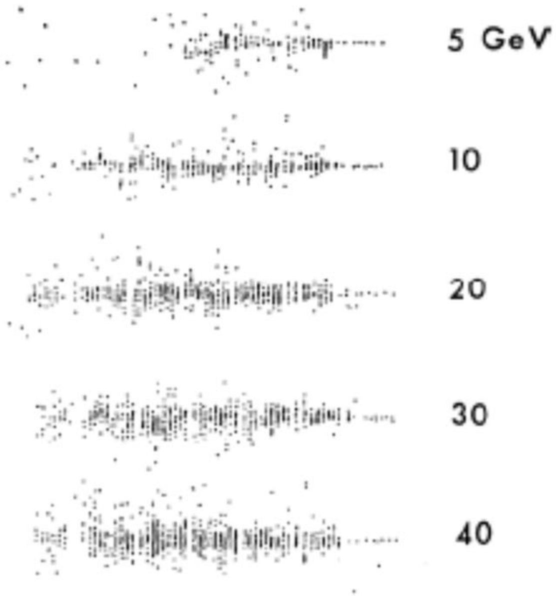

Hadron showers

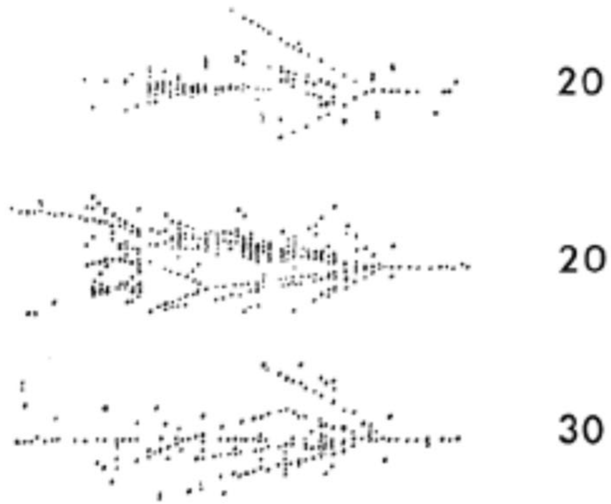

F.E. Taylor et al., IEEE NS 27(1980)30

O. Ullaland/2006

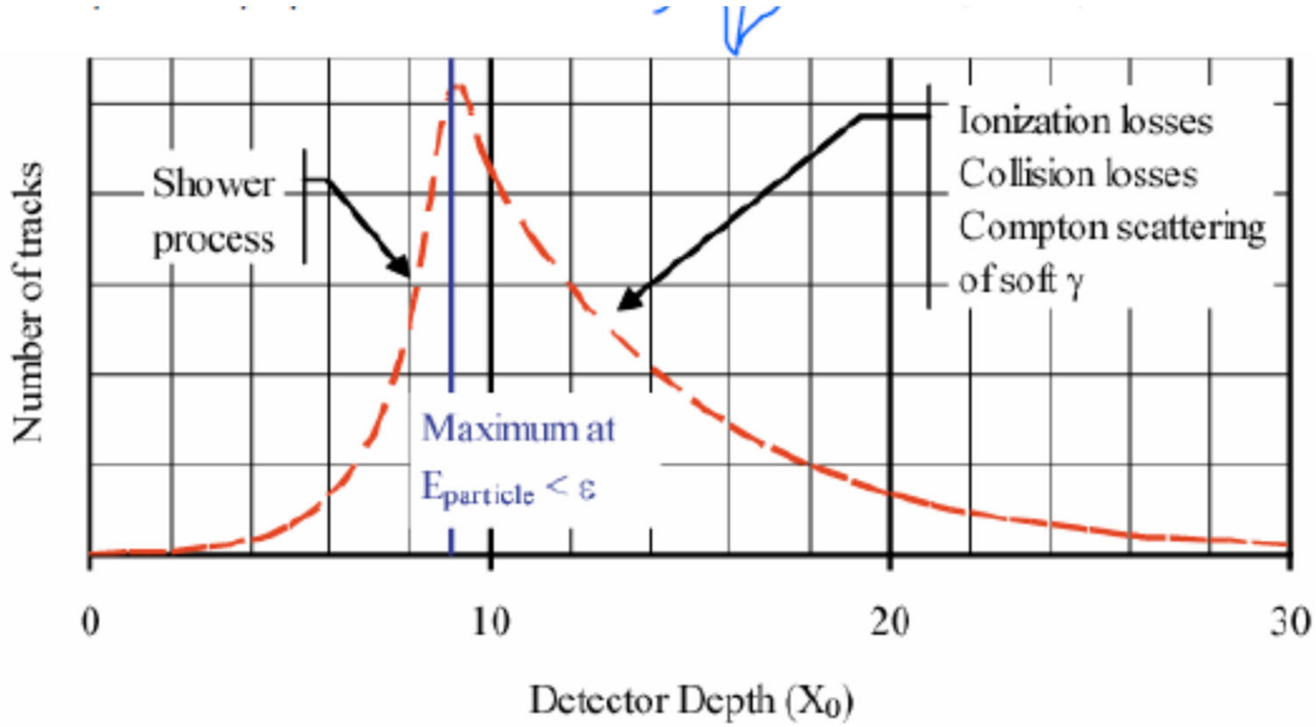

Number of tracks
Shower process
Ionization losses
Collision losses
Compton scattering of soft γ
Maximum at $E_{particle} < \varepsilon$
0
10
20
30
Detector Depth (X_0)

EM showers: longitudinal profile

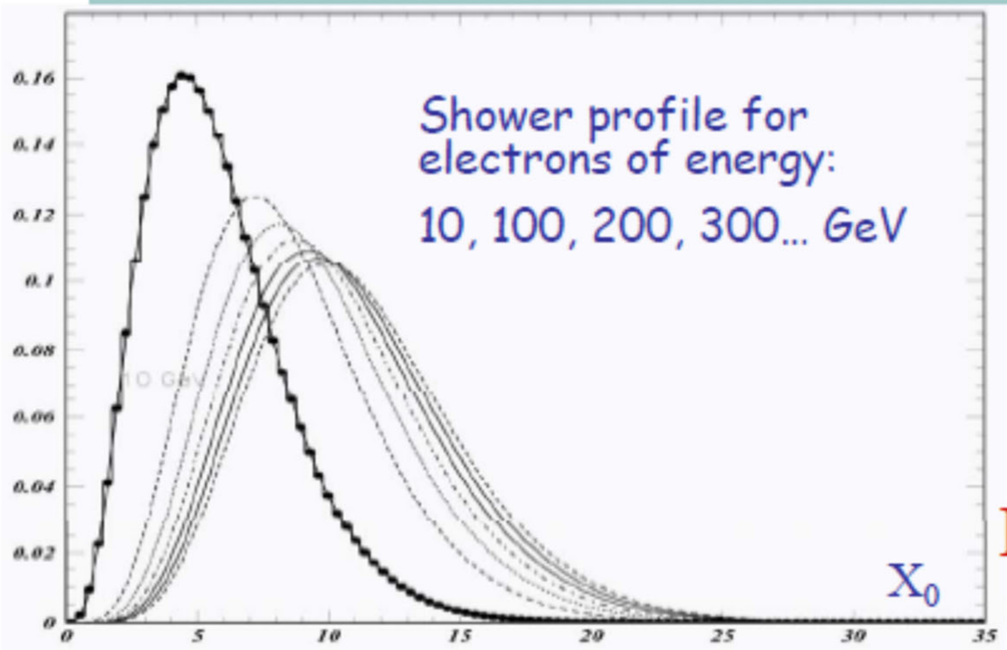

$t_{max} = 1.4 \ln(E_0/E_c)$

$N_{tot} \propto E_0/E_c$

Longitudinal containment:

$t_{95\%} = t_{max} + 0.08Z + 9.6$

$E_c \propto 1/Z$ ➡ •shower max •shower tail

Shower parametrization

$$\frac{dE}{dt} \propto t^{\alpha} e^{\beta t}$$

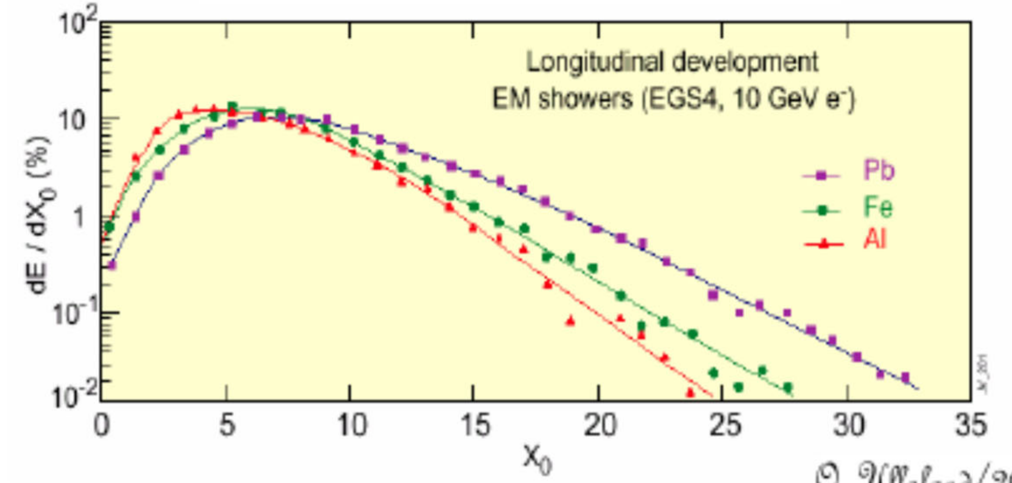

From M. Diemoz, Torino 3-02-05

O. Ullaland/2006

EM showers: transverse profile

Transverse shower profile

- Multiple scattering make electrons move away from shower axis
- Photons with energies in the region of minimal absorption can travel far away from shower axis

Molière radius sets transverse shower size, it gives the average lateral deflection of critical energy electrons after traversing $1X_0$

$$R_M = \frac{21\text{MeV}}{E_C} X_0$$

$$R_M \propto \frac{X_0}{E_C} \propto \frac{A}{Z} \left(Z >> 1\right)$$

75% E_0 within $1R_M$, 95% within $2R_M$, 99% within $3.5R_M$

20 GeV γ in copper (simulation)

charged particles only

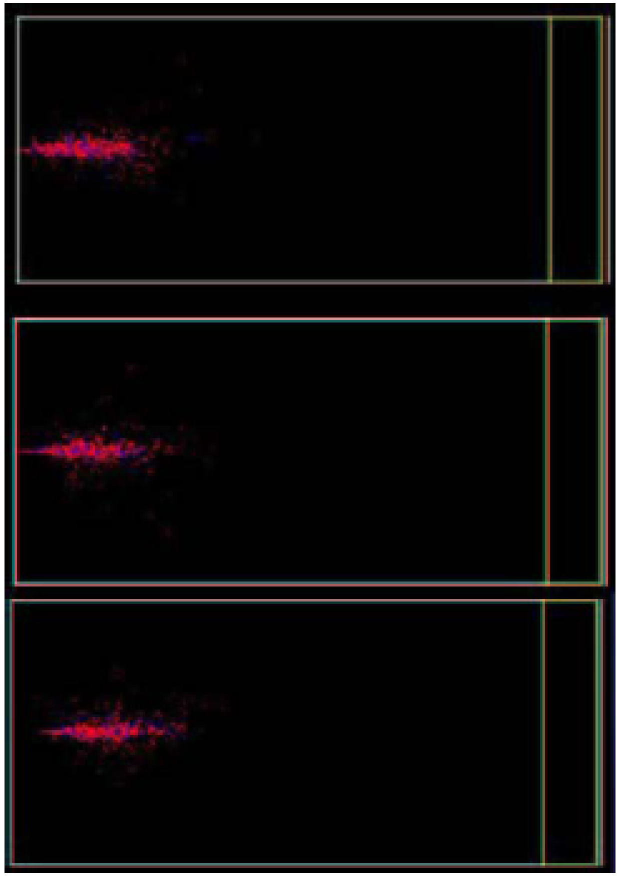

all particles

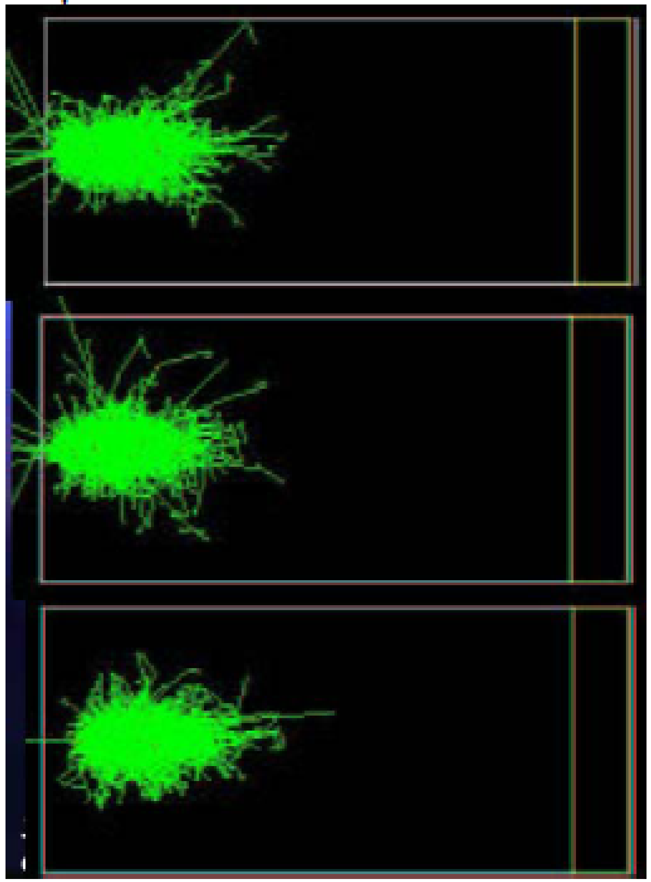

Electromagnetic calorimeters.

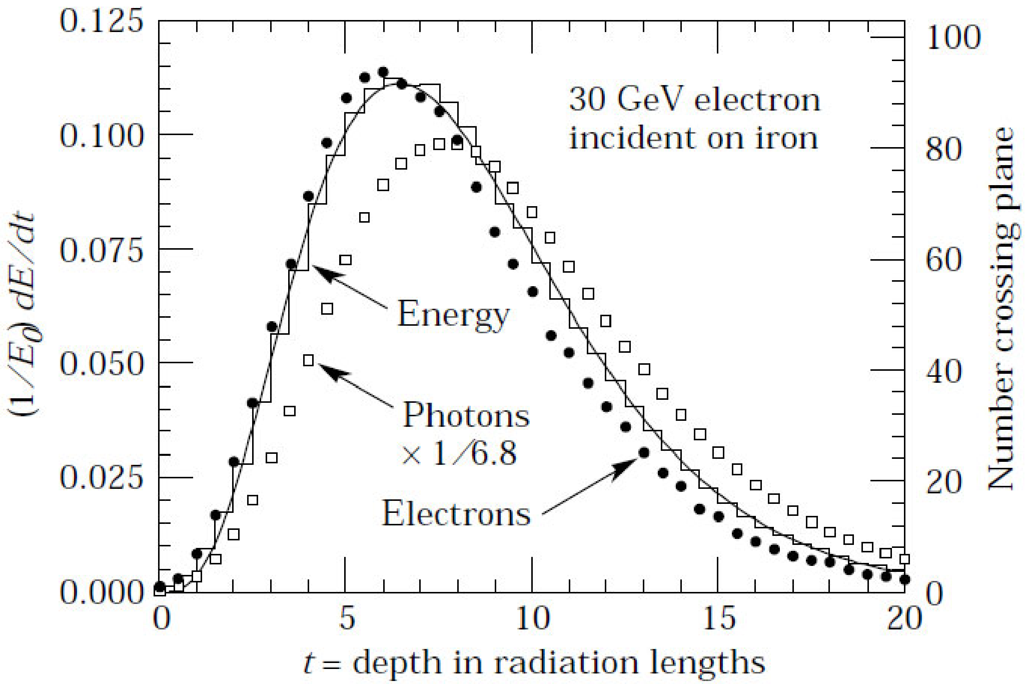

Figure 27.18: An EGS4 simulation of a 30 GeV electron-induced cascade in iron. The histogram shows fractional energy deposition per radiation length, and the curve is a gamma-function fit to the distribution. Circles indicate the number of electrons with total energy greater than 1.5 MeV crossing planes at $X_0/2$ intervals (scale on right) and the squares the number of photons with $E \geq 1.5$ MeV crossing the planes (scaled down to have same area as the electron distribution).

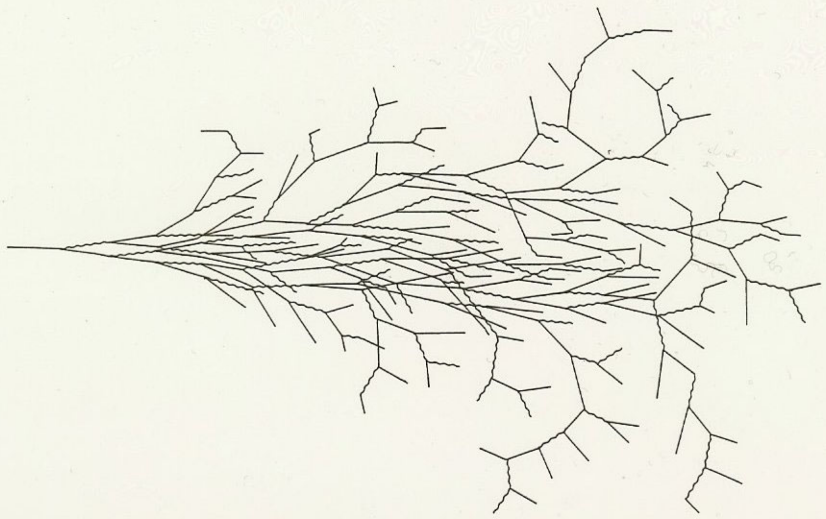

Fig. 7.20. Schematic representation of an electromagnetic cascade. The wavy lines are photons and the solid lines electrons or positrons.

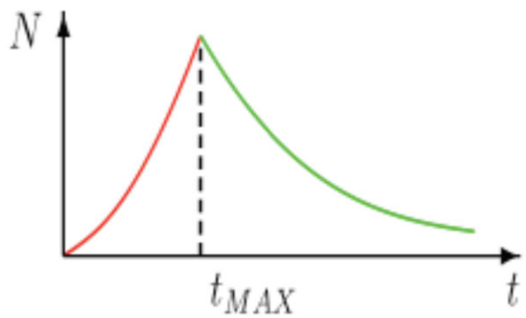

Figure 11.2 Shower profiles in lead. The number of electrons should be multiplied by a normalization factor of 0.79. (D. Müller, Phys. Rev. D 5: 2677, 1972.)

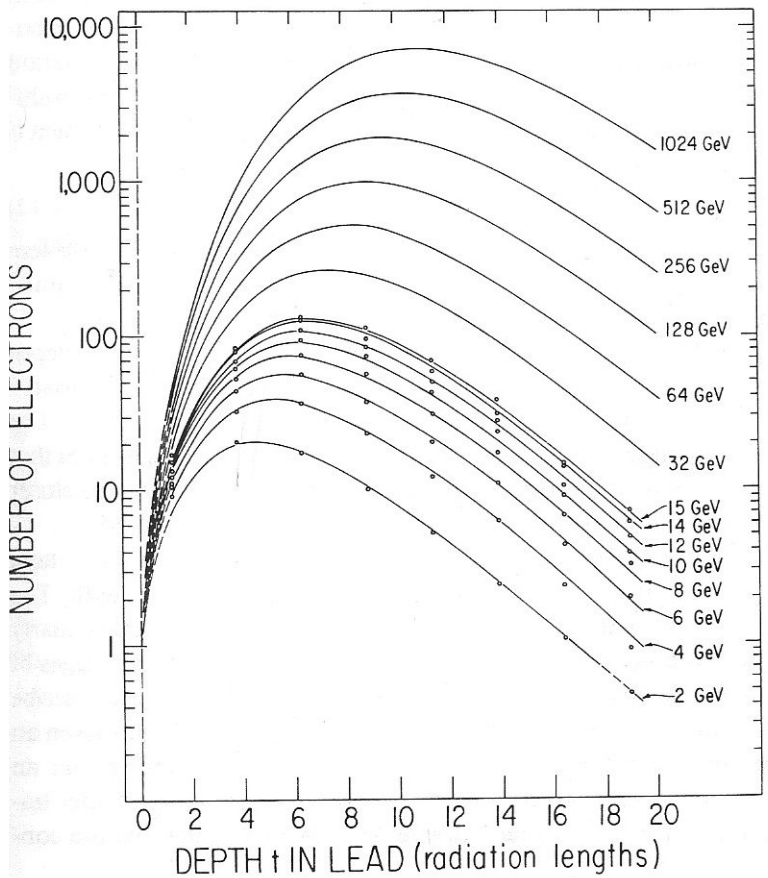

Figure 11.3 Longitudinal development of electromagnetic showers different materials. Right scale shows radii for 90% shower containmer (C. Fabjan and T. Ludlam, adapted with permission from the Annu Review of Nuclear and Particle Science, Vol. 32, © 1982 by Annu Reviews, Inc.)

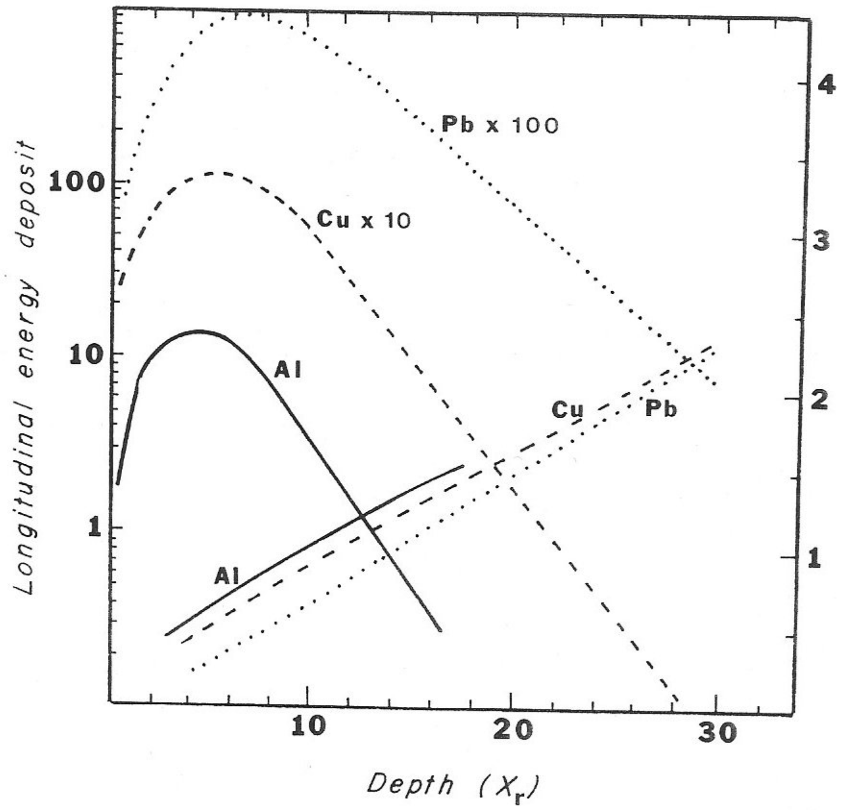

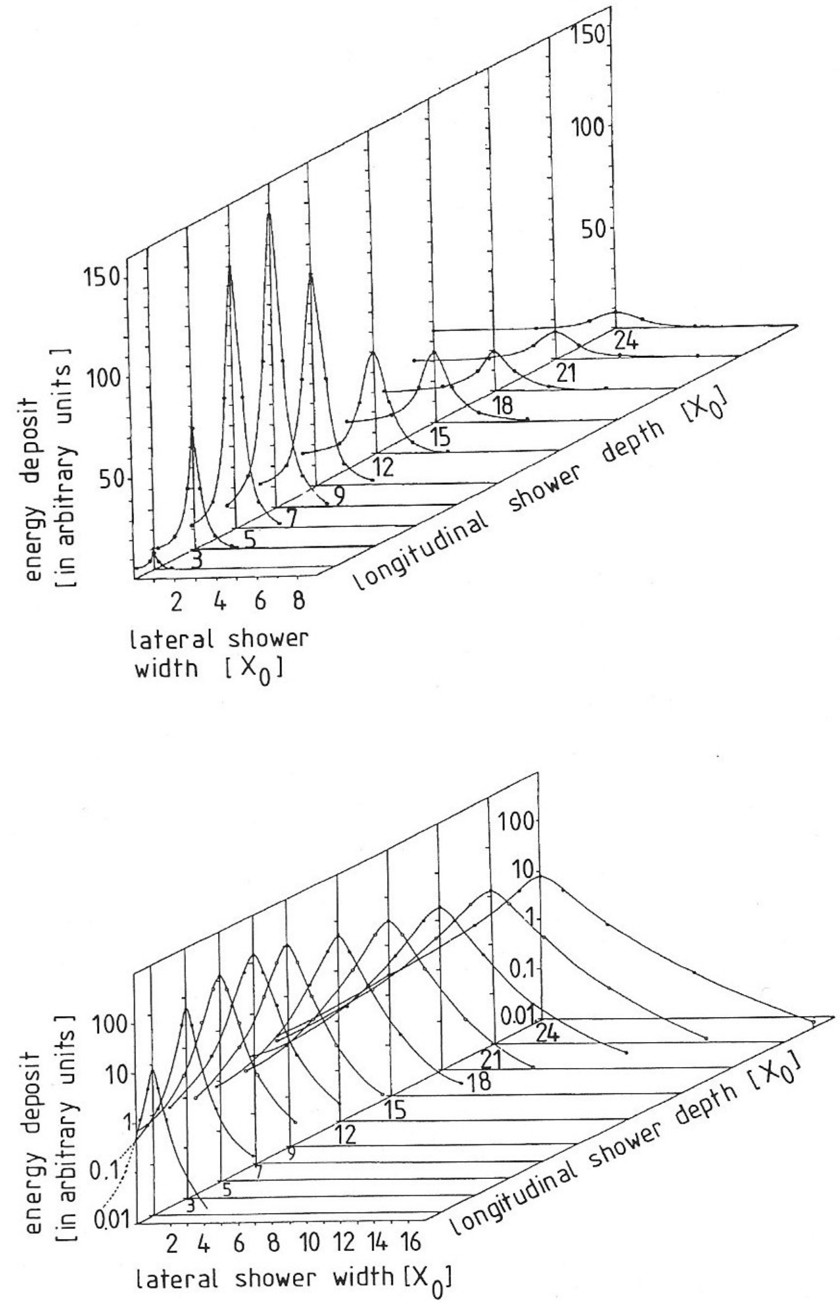

Fig. 7.23. Longitudinal and lateral development of an electron shower (6 GeV) in lead shown with linear and logarithmic scales (based on [504, 505]).

Electromagnetic calorimeters

- Basic readout types for sampling calorimeters

  - Metal-scintillator sandwich structure

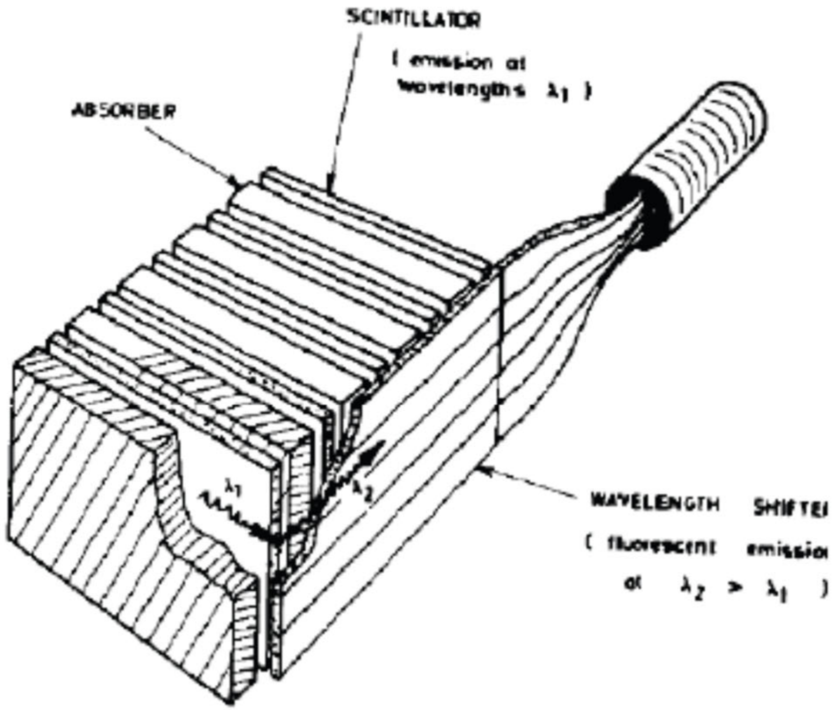

C. Fabjan and T. Ludlam, 1987

  - Metal-liquid argon ionization chamber

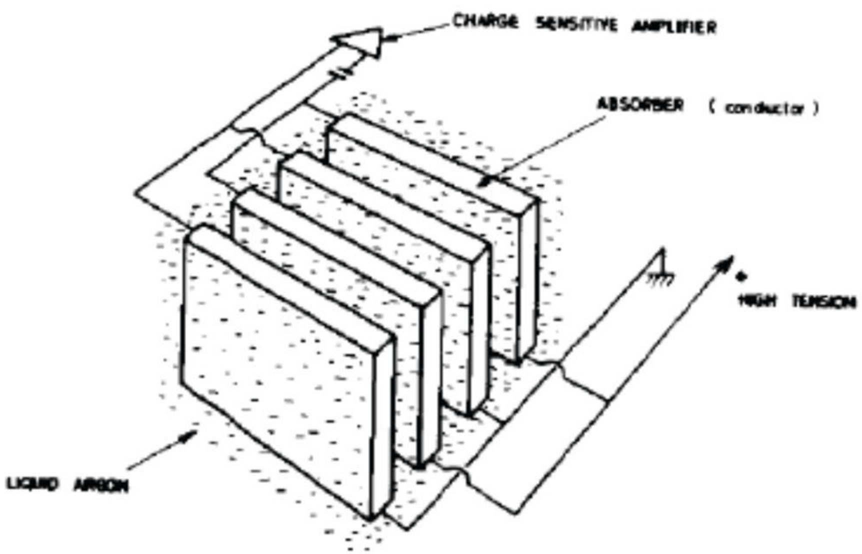

C. Fabjan and T. Ludlam, 1987

Electromagnetic showers

Energy resolution: Limitations

- Dead material effects

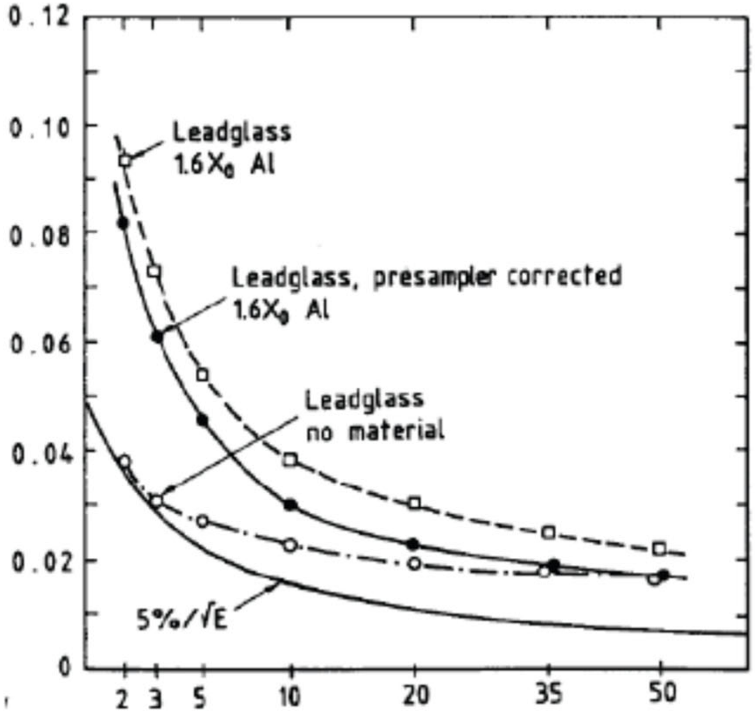

OPAL collaboration, C. Beard et al. NIM A 286 (1990) 117.

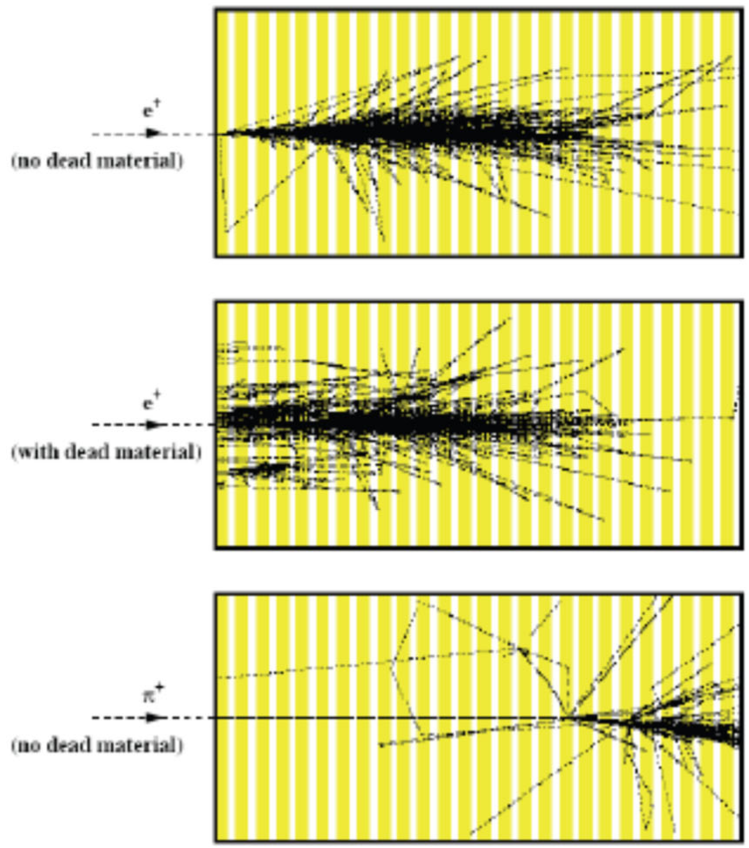

Hadronic showers

Hadronic shower development

- General comment: Complexity of of hadronic and nuclear processes produce multitude of effects that determine the functioning and performance of hadron calorimeters
  - Many channels compete in the development of hadronic showers
  - Larger variations in the deposited and visible energy
  - More complicated to optimize
- Sizeable electromagnetic (e) besides hadronic (h) shower contribution mainly from π^0 decay (1/3 of pions)
- Invisible energy due to delayed emitted photons in nuclear reactions, soft neutrons and binding energy
- Visible energy smaller for hadronic (h) than for electromagnetic (e) showers: Ratio of response e/h > 1
- Larger intrinsic fluctuations for hadronic than electromagnetic showers
- Improvements: Increase visible energy to get e/h=1: Compensation (Compensation for the loss of invisible energy)!
- Discussed instr. effects for e showers also hold for h showers

Step 1: Production of energetic hadrons with a mean free path given by the nuclear interaction length:

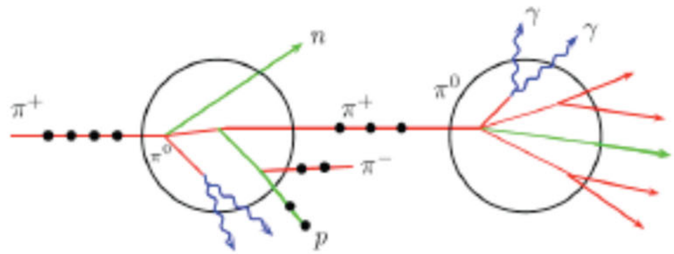

dE/dx nuclear cascade dE/dx nuclear cascade

Step 2: Hadronic collisions with material nuclei (significant part of the primary part of primary energy is consumed in nuclear processes):

Evaporation

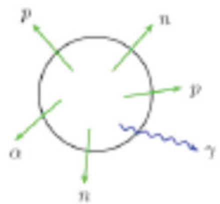

Evaporation followed by evaporation

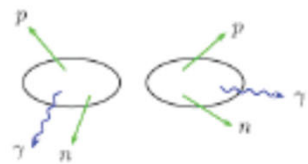

Processes contributing to the energy deposition in hadronic cal.

Table 11.2. *Average fractional energy deposition for a 10-GeV proton in an iron/liquid argon calorimeter*

Process	Percent of total
Secondary proton ionization	31.6
Electromagnetic cascade (π^0)	21.0
Nuclear binding energy plus neutrino energy	20.6
Secondary $\pi^{\pm}$ ionization	8.2
Neutrons with $E > 10$ MeV	4.9
Neutrons with $E < 10$ MeV	3.9
Residual nuclear excitation energy	3.7
$Z > 1$ ionization	2.4
Primary proton ionization	2.3
Other	1.4

Source: T. Gabriel and W. Schmidt, Oak Ridge National Laboratory report, ORNL/TM-5105, 1975.

Longitudinal distribution of energy in hadron calorimeter.

Fig. 6.6. Longitudinal distribution of energy deposited in a hadron calorimeter; Q_p is the energy deposited in counter p consisting of five layers with 2.5 cm iron and 0.5 cm scintillator each; $Q = \sum Q_p$. Measurements for π mesons of 15 GeV and 300 GeV [BL 82].

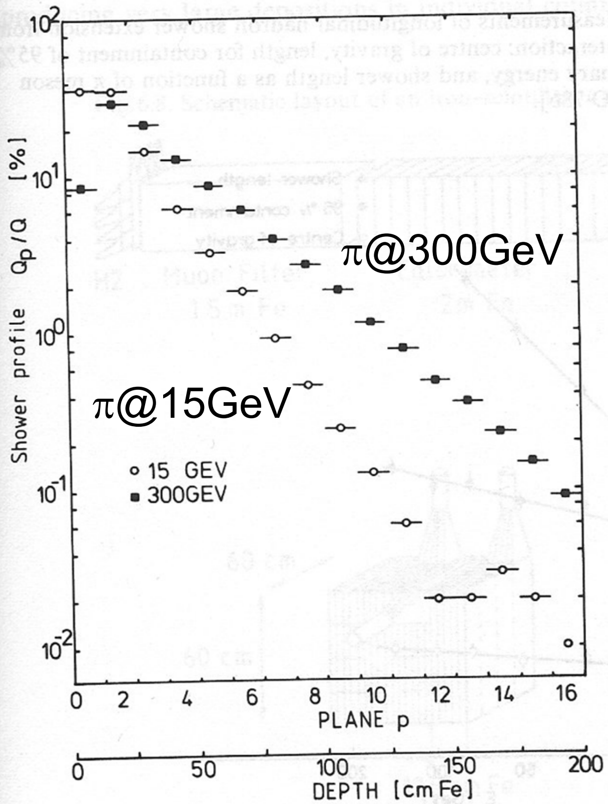

Energy resolution

Fig. 6.13. Relative energy resolution $\sigma(E)/E$ for different calorimeters; Fe (1.5 mm) and U (1.7 mm) from [FA 77]; Fe (25 mm) from [AB 81, BL 82].

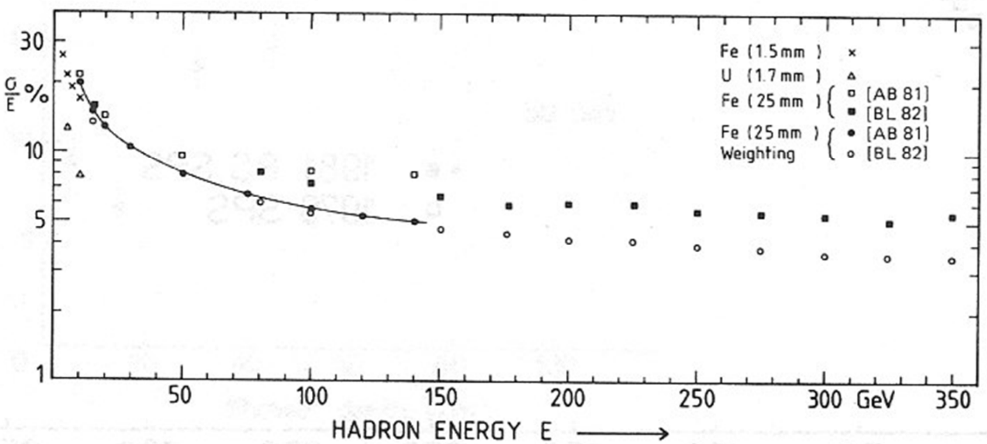

Dependence of resolution on sampling characteristics

Fig. 6.16. Reduced energy resolution $\sigma(E)/\sqrt{E(\text{GeV})}$ in units of (% $\sqrt{(\text{GeV})}$) as a function of sampling thickness of iron plates.

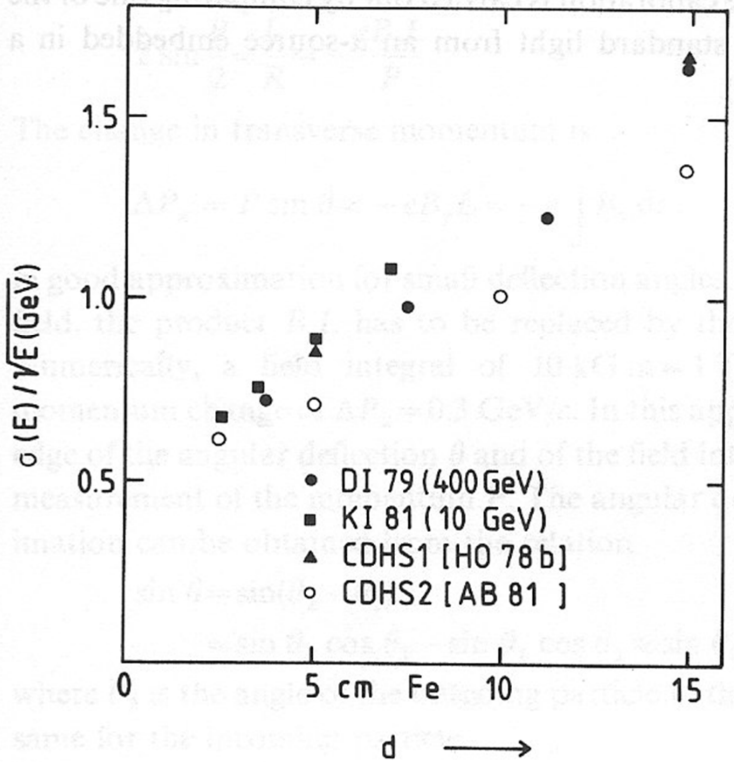

Technologies

Electromagnetic calorimeters

◆ ***Crystals***

(current calorimeters)	***CsI (Tl)***	$2.3\%/\sqrt[4]{E} \oplus 1.9\%$	*BaBar*
		$1.5\%/\sqrt[4]{E} \oplus 1.2\%$	*BELLE*
	$PbWO_4$	$2.8\%/\sqrt{E} \oplus 0.6\%$	*CMS*
		$3.3\%/\sqrt{E}$ *(low noise term)*	*ALICE*

◆ ***LAr/Pb*** *(accordion)*	$10\%/\sqrt{E} \oplus 0.7\%$	*ATLAS*
◆ ***Scint./Pb*** *(shashlik)*	$10\%/\sqrt{E} \oplus 1\%$	*LHCb*

Technologies

Hadron Calorimeters

♦ *Scint. / Brass (WLS readout)*	$\sim 100\% \sqrt{E} \oplus 4.5\%$	*CMS*
♦ *LAr / Brass*	$\sim 60\% \sqrt{E} \oplus 3\%$	*ATLAS (end-cap)*
♦ *Scint / Fe (WLS readout) (tiles oriented parallel to the beam)*	$\sim 50\% \sqrt{E} \oplus 3\%$	*ATLAS (barrel)*
♦ *Scint / Fe (WLS readout) (similar to ATLAS tile calorimeter, but planar geometry, 5.4 λ depth)*	$\sim 70\% \sqrt{E} \oplus 10\%$	*LHCb*

not compensated calorimeters
optimization of the jet energy resolution important !

Overview of LHCb ECAL

Two halves on chariots and electronics platform on top

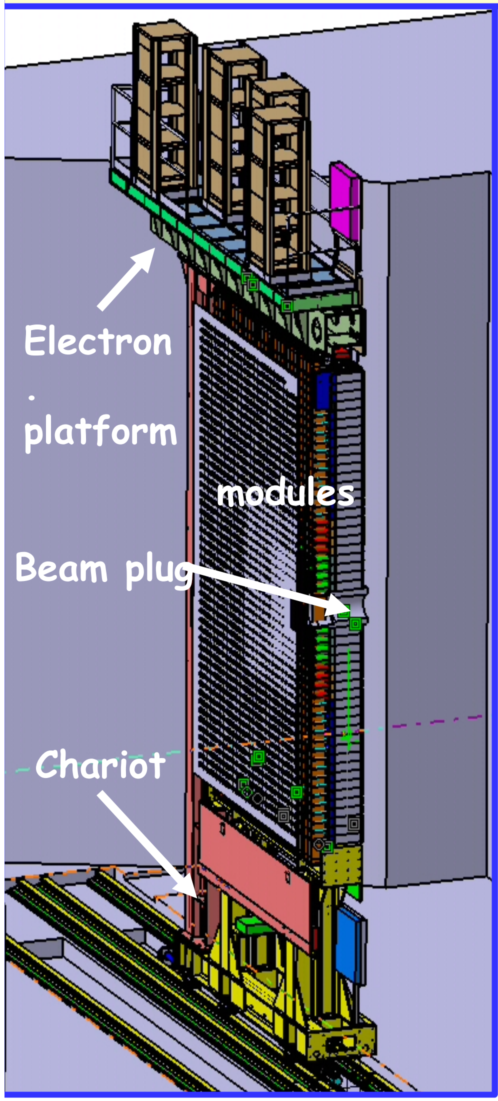

Fibres with loops

3312 shashlik modules with

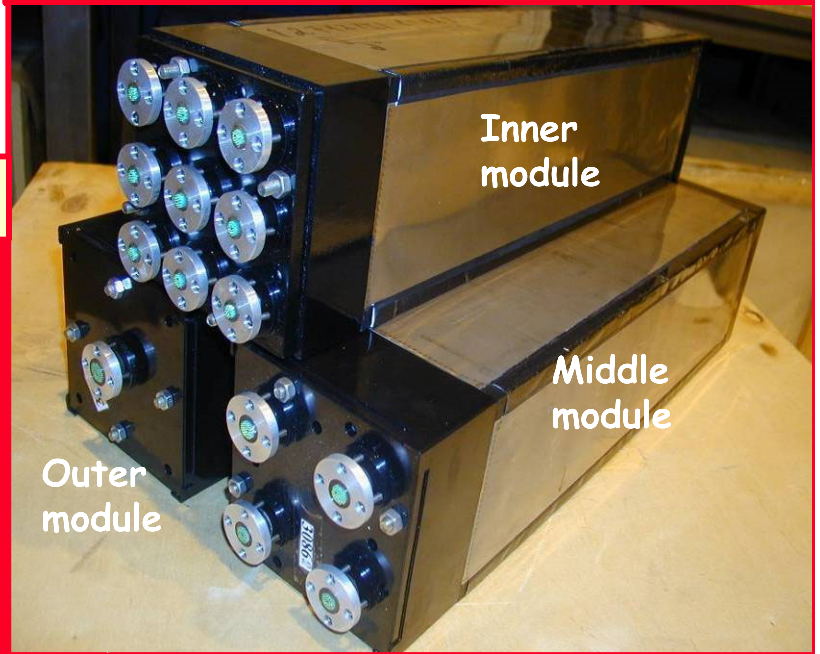

PMT and CW base

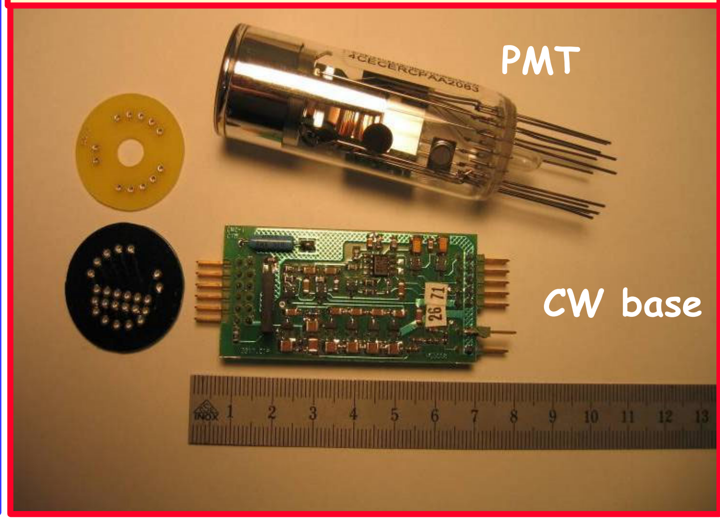

Scintillators, lead-plates, covers

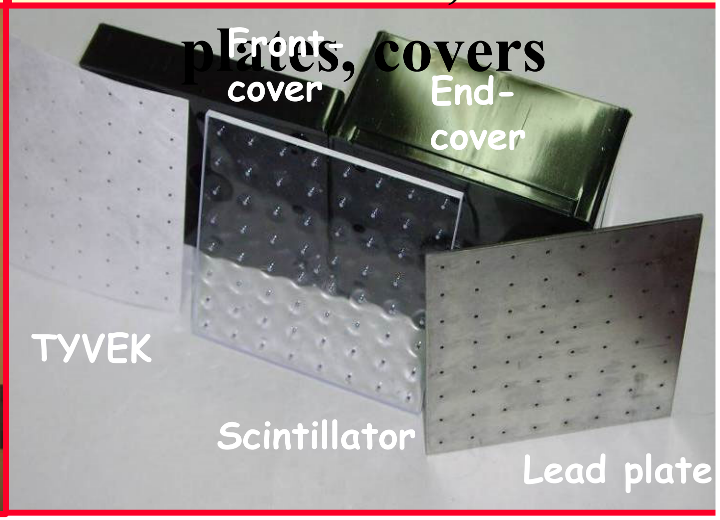

Overview of LHCb HCAL

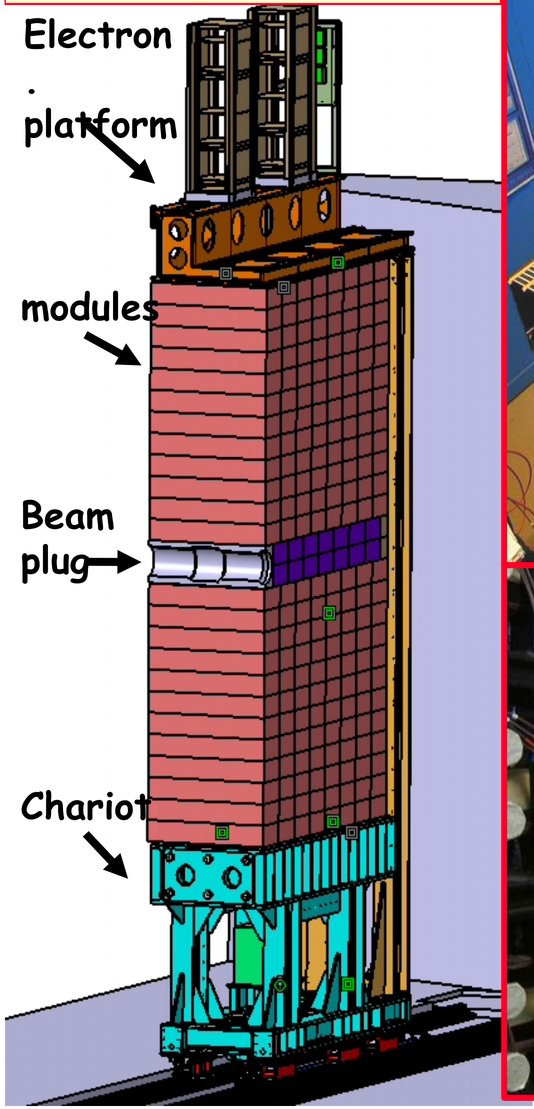

52 modules with longitudinal tiles

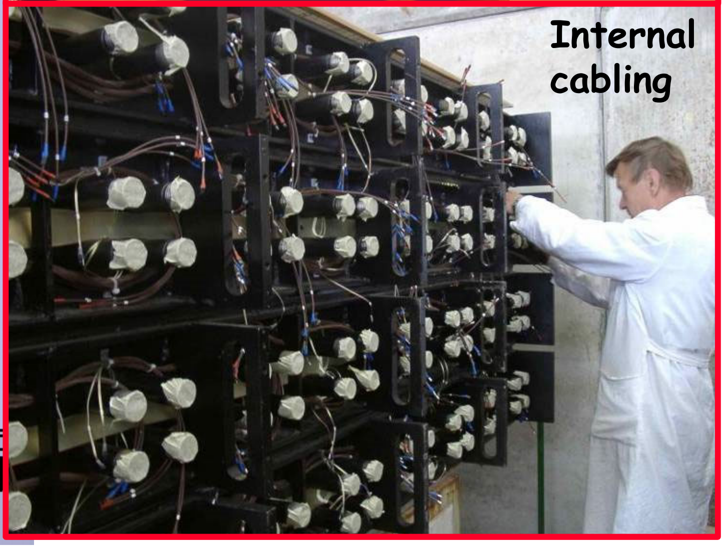

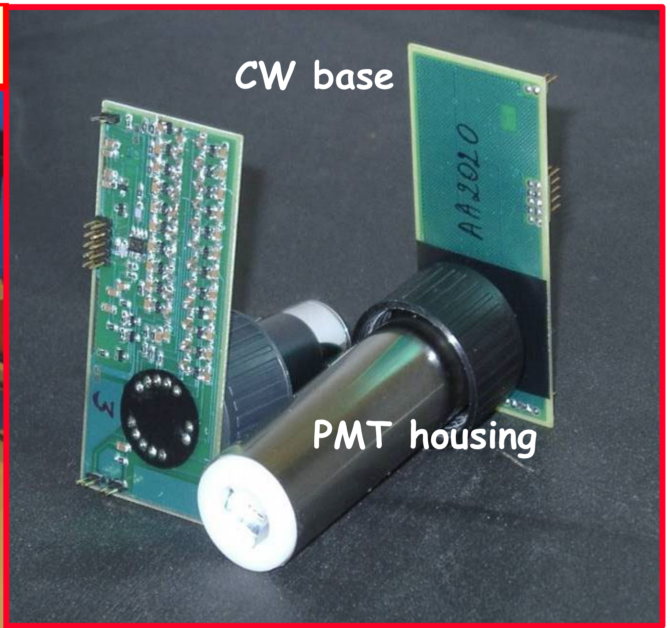

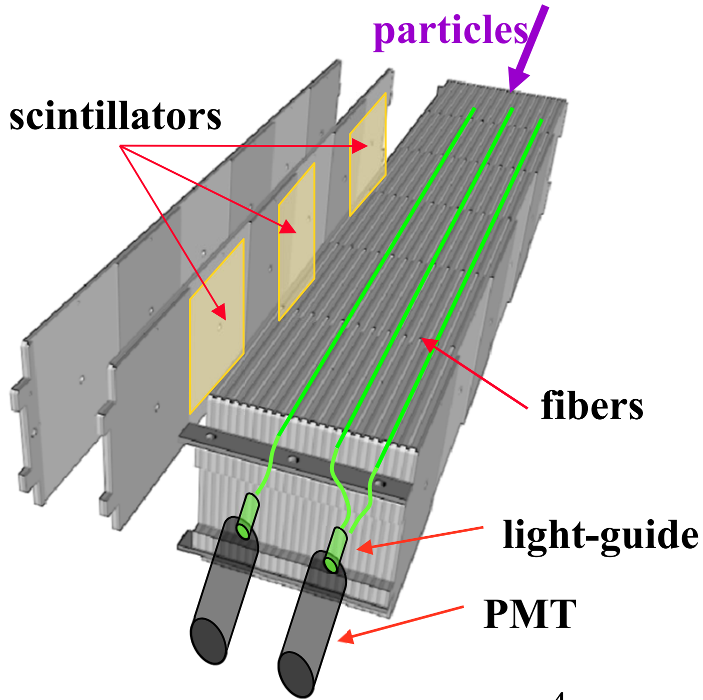

ALICE PHOS electromagnetic calorimeter

- **17920 PWO crystals**
- **distance to IP: 4.6m**
- **coverage in pseudo-rapidity:**
  $|\Delta\eta| < 0.12$
- **coverage in azimuthal angle:**
  $\Delta\Phi < 100°$
- **crystal size: $22\times22\times180$ mm^3**
- **Depth : $20X_0$**
- **photo readout: APD + CSP**
- **operating temperature: -25 ^{o}C**

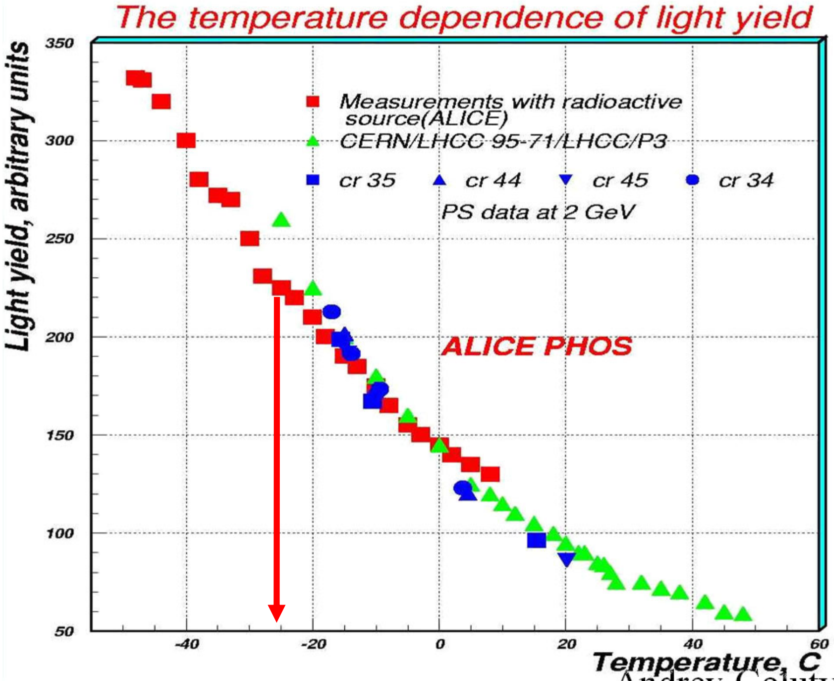

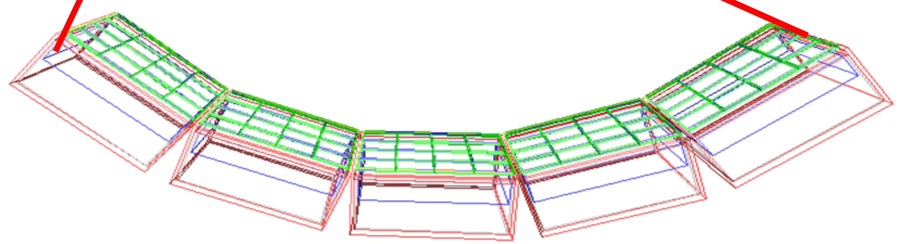

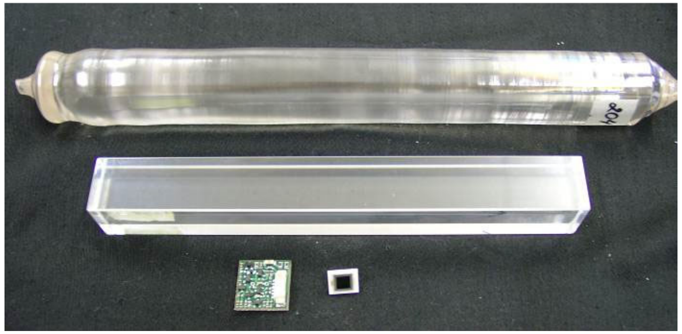

PHOS: *energy and position resolution* *(Daicu Zhou at QM2006)*

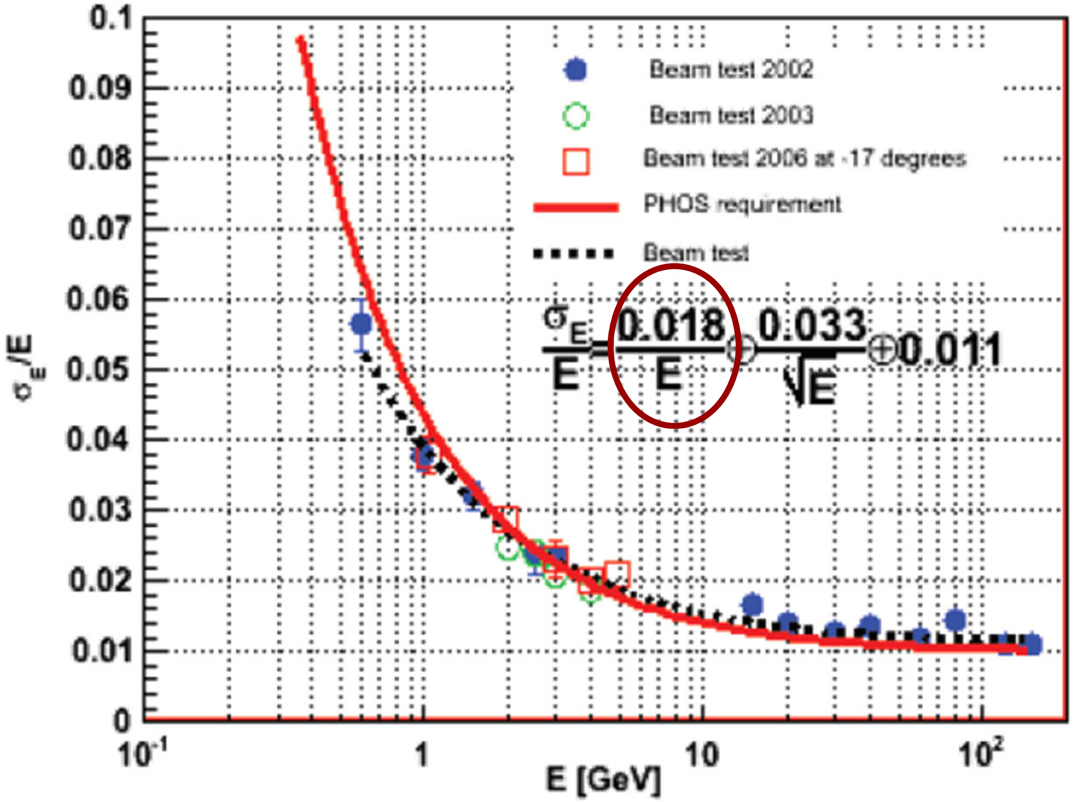

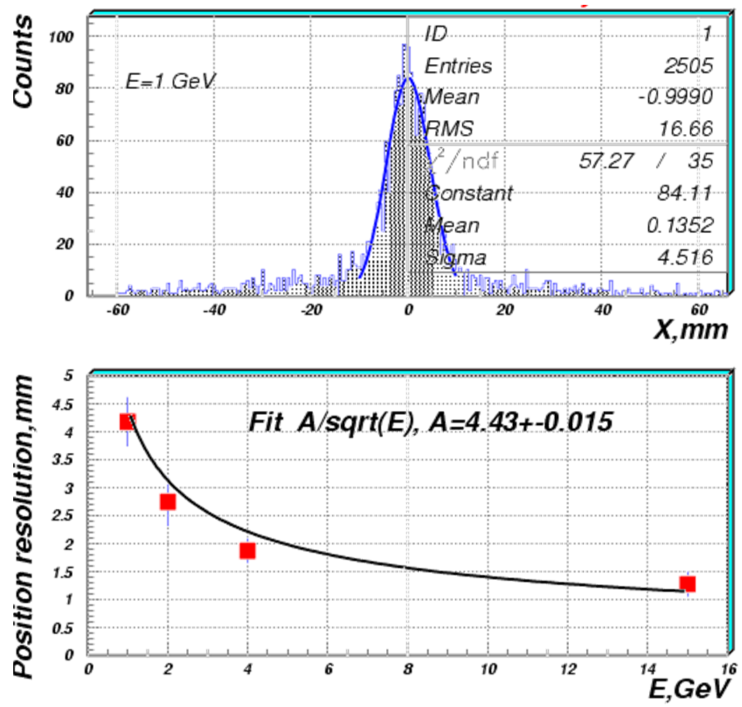

$\langle\sigma_x\rangle$ ~ 2.7mm @ 2 GeV

$\langle\sigma(E)/E\rangle$ ~ 3%, $\sigma(\sigma(E)/E)$ ~ 0.1% @ 2 GeV

PHOS: timing and mass resolution *(Daicu Zhou at QM2006)*

Timing resolution measurement with the electron beam. Standard start-stop method with an external trigger

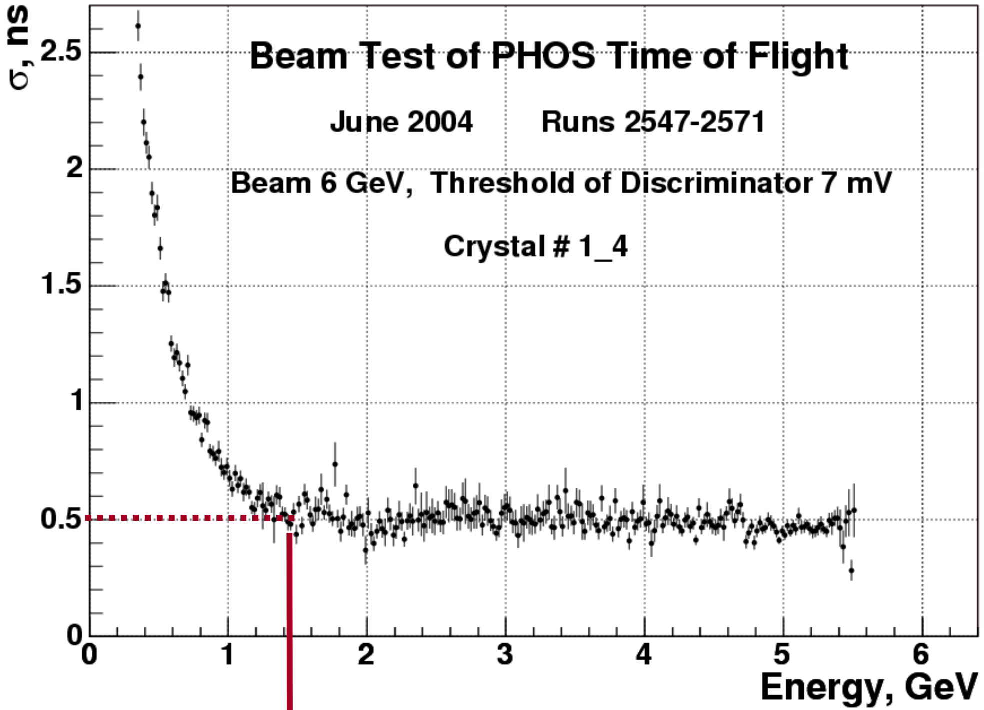

Invariant mass spect

$\pi^- + {}^{12}C \rightarrow \pi^0 + X \rightarrow 2\gamma + X$

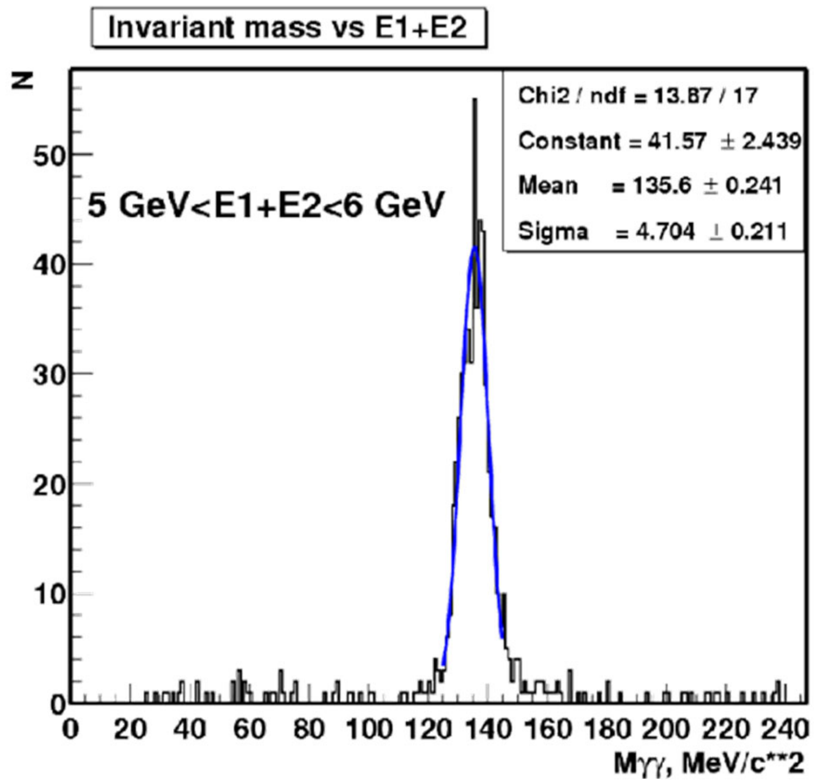

$\sigma \sim 0.5$ ns at $E > 1.5$ GeV

$\sigma(\pi^0) = 4.7$ MeV/c^2

π^0 is hard to see in ion-ion collisions

→ potential problem for intercalibration with data